Reduction of Chemical Reaction Networks Using Quasi-Integrals

Ronny Straube,[†] Dietrich Flockerzi,[‡] Stefan C. Müller,[†] and Marcus J. B. Hauser*,[†]

Abteilung Biophysik, Institut für Experimentelle Physik, Otto-von-Guericke Universität, Universitätsplatz 2, D-39106 Magdeburg, Germany, and Max-Planck-Institut für Dynamik komplexer technischer Systeme, Sandtorstr. 1, D-39106 Magdeburg, Germany

Received: September 24, 2004; In Final Form: November 2, 2004

We present a numerical method to identify possible candidates for quasi-stationary manifolds in complex reaction networks governed by systems of ordinary differential equations. Inspired by singular perturbation theory, we examine the ratios of certain components of the reaction rate vector. Those ratios that rapidly approach a nearly constant value define a slow manifold for the original flow in terms of quasi-integrals, that is, functions that are nearly constant along the trajectories. The dimensionality of the original system is thus effectively reduced without reliance on a priori knowledge of the different time scales in the system. We also demonstrate the relation of our approach to singular perturbation theory which, in its simplest form, is just the well-known quasi-steady-state approximation. In two case studies, we apply our method to oscillatory chemical systems: the 6-dimensional hemin−hydrogen peroxide−sulfite pH oscillator and a 10-dimensional mechanistic model for the peroxidase−oxidase (PO) reaction system. We conjecture that the presented method is especially suited for a straightforward reduction of higher dimensional dynamical systems where analytical methods fail to identify the different time scales associated with the slow invariant manifolds present in the system.

1. Introduction

Realistic modeling of complex reaction networks, such as those describing metabolism,[1,2] atmospheric chemistry,[3,4] and combustion,[5,6] usually requires the integration of quite large sets of equations which are systems of nonlinear ordinary differential equations (ODEs) provided that transport processes such as diffusion or convection are not taken into account.

We shall consider systems of the following form:

$$\dot{x} = f(x, k) \qquad f:\ \mathbb{R}^n \times \mathbb{R}^k \to \mathbb{R}^n \qquad (x, k) \in \mathbb{R}^n \times \mathbb{R}^k \tag{1}$$

where x and k denote the chemical species and all the parameters, respectively. For realistic reaction networks, the dimension n of system 1 can easily get in the order of hundreds (for instance, in the detailed description of combustion reactions[6] or the Belousov−Zhabotinsky reaction[7]). Even on fast computers, the numerical integration of such systems can be very time-consuming. Moreover, one is usually interested in investigating the system's behavior as one or more externally tunable parameters are continuously varied. This makes a straightforward integration of hundreds of equations inconvenient from a practical point of view. A reduction of complex reaction networks, on the other hand, may also be desirable for theoretical reasons:

First, one would like to identify those reaction steps and chemical species in a given mechanism that are necessary to generate a certain type of dynamics. While a general answer to this question is still unknown, there are already promising results for bistable[8] and oscillatory systems.[9,10] The main tools of investigation in this field are stoichiometric network analysis[11] and sensitivity analysis.[12] Both theoretical approaches have been successfully combined with principal component analysis to identify essential reaction steps in diverse systems such as the metabolism of red blood cells[13] and the Belousov−Zhabotinsky reaction.[14]

Second, chemical reactions naturally evolve on different time scales. Accordingly, their temporal evolution can be decomposed into a fast transient relaxation to lower dimensional invariant manifolds and a subsequent slow evolution on the union of these manifolds, which often still captures the interesting type of dynamics on experimentally accessible time scales. The mathematical description of such reaction networks leads to singularly perturbed systems for which a well developed theory exists.[15−17] As a result, a lower dimensional approximation to the original ODE system is obtained.

Meanwhile, several methods exploiting singular perturbation techniques have been proposed to simplify complex chemical reaction networks, such as lumping schemes[18] or the approximation of the invariant manifold based on a functional equation.[19] However, before these techniques may be successfully applied, one needs to identify the different time scales in the system. They usually show up as small dimensionless parameters in front of time derivatives of some of the phase space variables, indicating that these variables vary significantly only on very short time scales and henceforth follow instantaneously (algebraically) the dynamics of the slow degrees of freedom. The conventional strategy for searching for a small parameter is to introduce new dimensionless variables such that some combination of intrinsic system parameters becomes sufficiently small and subsequently may be used as a singular perturbation

* Corresponding author. E-mail: marcus.hauser@physik.uni-magdeburg.de.
[†] Otto-von-Guericke Universität.
[‡] Max-Planck-Institut für Dynamik komplexer technischer Systeme.

10.1021/jp045665s CCC: $30.25
Published on Web 12/30/2004

parameter. Clearly, this procedure becomes a formidable task in more complex reaction networks and other methods are required, for example, the method of computational singular perturbation.[20] Furthermore, the rescaling procedure is not free of ambiguity in choosing the "right" scales,[21] and if the rescaled phase space variables are not bounded from above and below, then the rescaled kinetic parameters do not provide any indication of whether the corresponding reaction step is slow or fast. Thus, one is often guided by chemical intuition or experimental expertise in grouping the individual reactions according to slow and fast steps. Once the different time scales of a system are known, it is more or less straightforward to apply singular perturbation techniques to obtain a lower dimensional approximation of the original dynamics on a slow manifold of the system.

In the present article, we propose a method based on the successful identification of a certain class of quasi-integrals which arise as ratios of those components of the reaction rate vector which are nearly constant along the trajectories of ODE system 1. As a result, possible slow manifolds for a given reaction network are obtained without the aforementioned prerequisites, that is, necessity of rescaling and chemical intuition. Thereafter, we use the method of parameter embedding as described by Stiefenhofer[22] to test whether the quasi-integrals that we found with our method truly define a slow manifold for the original system. We shall now briefly outline this method.

The embedding method relies on some a priori knowledge of the order of magnitude of individual reaction steps. Having identified the fast reaction steps, one may embed ODE system 1 in an ϵ-dependent family of ODE systems of the following form (the parameters k are omitted for convenience):

$$\dot{y} = h(y, z) \qquad y \in \mathbb{R}^{n-m}$$

$$\epsilon\dot{z} = r(y, z) + \epsilon g(y, z) \qquad z \in \mathbb{R}^{m} \tag{2}$$

Here, we have collected the fast reaction steps into the components of the vector-valued function $r(y, z)$. For $\epsilon \equiv 1$, ODE system 2 coincides with (1), provided the identifications $x \equiv (y, z) \in \mathbb{R}^{n-m} \times \mathbb{R}^m$ and $f \equiv (h, r+g) \in \mathbb{R}^{n-m} \times \mathbb{R}^m$ are made and the equations in (1) are ordered such that the last m of them contain the fast reaction steps. One can now study the behavior of ODE system 2 for parameter values ϵ different from 1. Of particular interest is the case when $\epsilon \ll 1$, because then (2) becomes a singularly perturbed system for which a slow manifold of the form $z = \psi(y, \epsilon) = \tilde{z}(y) + \mathcal{O}(\epsilon)$ may exist. In the limit $\epsilon \to 0$, the slow manifold can be approximated by the quasi-stationary manifold $z = \tilde{z}(y)$, which is the solution of the algebraic equation $r(y, z) = 0$. This can be seen by introducing a fast time scale τ according to $t = \epsilon\tau$. Hereafter, ODE system 2 reads

$$y' = \epsilon h(y, z) \qquad y \in \mathbb{R}^{n-m}$$

$$z' = r(y, z) + \epsilon g(y, z) \qquad z \in \mathbb{R}^{m} \tag{3}$$

where the prime sign denotes derivatives with respect to τ. If $\epsilon \neq 0$, the two systems (2 and 3) are completely equivalent. In the limit $\epsilon \to 0$, however, this equivalence is lost. From (3), one obtains an approximate equation for the dynamical behavior of the original system on the time scale τ:

$$z' = r(y, z) \tag{4}$$

This equation is called the fast subsystem, and its stationary states define the quasi-stationary manifold for the flow of the original ODE system (1). Since the slow variables y are assumed to vary significantly only on time scales $t \gg \tau$, they are to be treated as constants and act as parameters in (4). The long-term behavior of the original system on the quasi-stationary manifold is described in terms of the slow subsystem which is obtained from (2) in the limit $\epsilon \to 0$:

$$\dot{y} = h(y, z)$$

$$z = \tilde{z}(y) \tag{5}$$

The conditions under which these approximations are valid have been elaborated by Fenichel[15] and will be presented in the next section when we discuss how quasi-integrals and singular perturbation theory are related.

Finally, we study by numerical investigations whether trajectories of the original system (2) (corresponding to $\epsilon = 1$) smoothly deform into trajectories of the reduced slow subsystem (5) (corresponding to $\epsilon = 0$). (This procedure corresponds to the homotopy argument used by Stiefenhofer.[22]) In such a case, the fast reactions indeed define a quasi-stationary manifold and the reduction process is a posteriori justified. In this sense, the method of quasi-integrals may serve as a supplement to existing methods which rely on prior knowledge of time scales.

In the following section, we introduce the method of quasi-integrals in detail and elucidate its connection to singular perturbation theory. After a brief description of the numerical methods, we present two case studies in which we apply our method to oscillatory chemical systems. First, we demonstrate in detail how a 6-dimensional enzyme model system can be reduced to a 3-dimensional system while maintaining its local bifurcation structure. The second case study focuses on the peroxidase−oxidase (PO) reaction. This 10-dimensional reaction system can be reduced to 6 dimensions, while most of the qualitative features of the original model are retained. Finally, we discuss the scope and limitations of the introduced method.

2. The Connection between Quasi-Integrals and Singularly Perturbed Systems

In the following, we assume that the reaction network under consideration is of mass-action type, since most chemical networks belong to this class. Moreover, there is a "natural" choice for the class of quasi-integral manifolds in such systems to be looked for. Consequently, we may represent the vector field in system 1 as

$$f(x, k) = \mathbf{C}\cdot\mathbf{R}(x, k) \tag{6}$$

where the components of the reaction rate vector $\mathbf{R}(x, k)$ are given by

$$R_i(x, k) = k_i \prod_j x_j^{\kappa_{ji}} \qquad i = 1, \ldots, r \text{ and } j = 1, \ldots, n$$

$\mathbf{C}$ and κ denote the matrix of stoichiometric coefficients and the kinetic matrix, respectively. While the former encodes the network topology, the latter contains the kinetic information of each individual reaction step. Both matrices have as many rows as there are chemical species (n) and as many columns as there are individual reaction steps (r) in the network. Due to (6), the components of the vector field f that appear on the right-hand side of ODE system 1 are linear combinations of components of the reaction rate vector R, that is,

$$\dot{x}_l = f_l(x, k) = \sum_{i=1}^{r} C_{li} R_i(x, k) \qquad l = 1, \ldots, n \tag{7}$$

Now, we claim that whenever a ratio

$$I_{ij}^{l} = \frac{C_{li}R_i(x(t), k)}{C_{lj}R_j(x(t), k)} \sim -1 \tag{8}$$

approaches approximately the constant value -1 along the trajectories $x(t)$ for a certain combination of indices $l \in \{1, \ldots, n\}$, $i, j \in \{1, \ldots, r\}$, we have found a possible candidate, I_{ij}^{l}, of a quasi-integral which defines a quasi-stationary manifold for ODE system 7. Equation 8 may also be looked at in the following way:

$$\frac{R_i(x(t), k)}{R_j(x(t), k)} \sim -\frac{C_{lj}}{C_{li}} \tag{9}$$

which shows that for quasi-integrals the kinetics of the reaction network represented by the left-hand side approximately equals the topological constraints given by the stoichiometric coefficients on the right-hand side. Alternatively, eq 8 may be written in the form

$$\tilde{I}_{ij}^{l} = C_{li}R_i(x(t), k) + C_{lj}R_j(x(t), k) \sim 0 \tag{10}$$

showing that we are actually searching for reaction steps that balance each other along the trajectories. Consequently, one has to consider only such combinations R_i, R_j for which $\mathrm{sign}(C_{lj}) = -\mathrm{sign}(C_{li})$ is fulfilled. This also explains the choice of "-1" on the right-hand side of eq 8.

Of course, one can easily extend this definition and try to balance more than two reaction steps, for instance,

$$\tilde{I}_{ijk}^{l} = C_{li}R_i(x(t), k) + C_{lj}R_j(x(t), k) + C_{lk}R_k(x(t), k) \sim 0 \tag{11}$$

In this case, we would consider quasi-integrals of the following form:

$$I_{ijk}^{l} = \frac{C_{li}R_i(x(t), k) + C_{lk}R_k(x(t), k)}{C_{lj}R_j(x(t), k)} \sim -1 \tag{12}$$

provided that, for example, $\mathrm{sign}(C_{li}) = \mathrm{sign}(C_{lk}) = -\mathrm{sign}(C_{lj})$ holds. Indeed, for the peroxidase−oxidase system, we find two quasi-integrals of this form (see the Case Studies section). The motivation for the particular choice of the functions I_{ij}^{l} (eq 8) and their alternative representations $\tilde{I}_{ij}^{l}$ (eq 10) becomes clear when we draw the connection to singular perturbation theory. Therefore, we now review some aspects of this theory that are important for our argumentation.

Singularly perturbed systems admit the following canonical representation:

$$\begin{aligned} \dot{y} &= h(y, z, \epsilon) \qquad y \in \mathbb{R}^{n-m} \\ \epsilon\dot{z} &= g(y, z, \epsilon) \qquad z \in \mathbb{R}^{m} \end{aligned} \tag{13}$$

where ϵ is a sufficiently small dimensionless parameter. Now, we assume that the function g can be decomposed as $g(y, z, \epsilon) = r(y, z) + \epsilon g_1(y, z, \epsilon)$. Then, the "slow" subsystem (in the limit $\epsilon \to 0$) is described by the differential−algebraic system

$$\begin{aligned} \dot{y} &= h(y, z, 0) \\ 0 &= r(y, z) \end{aligned} \tag{14}$$

whenever the second equation in (14) defines a smooth manifold of the form $z = \tilde{z}(y)$. Furthermore, this manifold is required to be normally attracting in the following sense: the real parts of the eigenvalues of

$$D_z r(y, \tilde{z}(y)) \tag{15}$$

are negative and bounded away from 0 for y belonging to a compact region in $\mathbb{R}^{n-m}$. $D_z r(y, \tilde{z}(y))$ denotes the Jacobian of the fast subsystem (in the limit $\epsilon \to 0$)

$$\frac{dy}{d\tau} = 0, \quad \frac{dz}{d\tau} = r(y, z), \quad t = \epsilon\tau \tag{16}$$

where the slow variables y are to be treated as parameters. Under these conditions, the asymptotic dynamics of the n-dimensional system (13) can be approximated for sufficiently small ϵ to lowest order by

$$\dot{y} = h(y, \tilde{z}(y), 0) \tag{17}$$

which is now an ODE system of dimension $n - m$. Equation 17 is the zeroth order approximation with respect to the singular perturbation parameter ϵ and is well-known as the quasi-steady-state approximation (QSSA).

When comparing (7) and (10) with (14), the motivation for our choice of the nonlinear functions I_{ij}^{l} in (8) becomes apparent, since if we truly wish eq 10 to define a quasi-stationary manifold in the sense of the second equation of (14), we have to make the following identification for the components of the vector field r:

$$r_{ij}^{l} \equiv \tilde{I}_{ij}^{l} = C_{li}R_i(x, k) + C_{lj}R_j(x, k) \tag{18}$$

In this case, (8) is a necessary condition for the existence of a quasi-stationary manifold defined by (10), which seems to be a natural class of slow manifolds that one can expect in chemical reaction networks of mass-action type. Alternatively, r may also be identified with $\tilde{I}_{ijk}^{l}$ depending on how many reaction steps balance each other. The condition (8) would also be sufficient if the two reaction rates, R_i and R_j, appearing in (10) dominated in magnitude over the others (which were absorbed into the definition of g_1). However, this requirement is automatically ensured by our method, since we examine the ratios of the form of (8) and (12) along the numerical integration curves. Ratios deviating notably from the value -1 are composed of reaction steps that do not balance each other along the integral curves or that do not dominate over the other reaction steps in a given rate equation. Thus, the difficulty in identifying a quasi-integral is shifted to the task of deciding whether a given ratio of the form of (8) or (12) is "nearly" equal to -1. As will be shown in the two case studies later on, we have no difficulty finding the quasi-integrals there. Nevertheless, it would be of great benefit to have a more rigorous measure of the loose statement "nearly constant", especially for identifying quasi-integrals in higher dimensional reaction networks. We will come back to this point in the Discussion, where we also give a more formal working definition of a quasi-integral which may serve as a starting point for their automatic detection.

Thus, we arrive at a finite algorithm to probe a given reaction mechanism for the existence of equilibrating reaction steps which can be summarized in the following three steps: First, integrate ODE system 1 over a sufficiently long time interval to obtain the trajectories for parameter values where the interesting asymptotic kind of dynamics is observed. Second, check whether quasi-integrals of the form of (8) or (12) exist. Third, apply available singular perturbation techniques to reduce the number of dynamical degrees of freedom. In the present

TABLE 1: Rate Constants and Inflow Stream Concentrations for the Hemin System (eq 20)

$k_1 = 0.2\ M^{-1}\cdot s^{-1}$	$k_2 = 1.5\ M^{-1}\cdot s^{-1}$	$k_3 = 8.5 \times 10^6\ M^{-2}\cdot s^{-1}$	$k_4 = 1000\ s^{-1}$
$k_5 = 10^{10}\ M^{-1}\cdot s^{-1}$	$k_6 = 0.011\ s^{-1}$	$k_7 = 2.5 \times 10^4\ M^{-1}\cdot s^{-1}$	$k_8 = 1.9 \times 10^{-4}\ s^{-1}$
$x_1^0 = 0.025\ M$	$x_2^0 = 0.045\ M$	$x_4^0 = 2.2 \times 10^{-4}\ M$	$x_5^0 = 3 \times 10^{-4}\ M$

article, we shall only make use of the QSSA to demonstrate the general applicability of our method.

3. Methods

The numerical integration of the ODE systems for our case studies in the next section (the hemin and the PO system) were done using the software package XPPAUT.[23] Since the reaction rates in the considered chemical networks vary over several orders of magnitude, we chose the "STIFF" integration algorithm with a tolerance of 10^{-5} to guarantee numerical stability. In addition, the equations were rescaled such that the maximal amplitude of the rescaled variables was of order unity. Nevertheless, the ODE system describing the PO reaction remained numerically very sensitive to slight changes in the concentrations of four of its species. In particular, we were not able to reach a stationary state. Even after very long integration times, the concentrations of these four species kept fluctuating from the fifth decimal digit on, which indicates strong correlations between them. This is probably due to the fact that, unlike the hemin system, the reaction mechanism of the PO system is entirely composed of irreversible reaction steps. The aforementioned problem not only occurs in the original 10-dimensional ODE system but persists in all of its reduced versions, too.

The method of numerical continuation (e.g., ref 24) was used for the hemin system to compare the original as well as the reduced ODE systems according to their local bifurcations. Continuation calculations were always started from a stable fixed point in the low pH region at pH $\sim$ 5.5, which we obtained by numerical integration of the corresponding ODE system from zero initial conditions. The parameter region, where the stable fixed point is reached, had to be tested in several runs. We found $k_0 = 1 \times 10^{-4}\ s^{-1}$ to be a suitable starting value.

Bifurcation diagrams for the peroxidase−oxidase system were obtained by computing the asymptotic dynamics of individual trajectories over the whole parameter range ($k_{12} = 1.00 \times 10^{-7}\ s^{-1}$, ... , $1.34 \times 10^{-7}\ s^{-1}$). For each parameter value, we discarded a transient of 35 000 time steps and recorded the successive maxima of the peroxidase compound III (coIII) concentration over the next 15 000 time steps. The run for the first parameter value of each simulation was always started from fixed initial conditions. For subsequent runs of the same simulation, but for other parameter values, we used the final concentrations of the preceding run as new initial conditions. It is thus possible to monitor the evolution of attractors as a parameter is almost continuously varied, provided the parameter step size is suitably adapted. We chose a step size of 10^{-3}. When interpreting these bifurcation diagrams, one has to take into account that they are topologically equivalent to a Poincaré map where the cutting section in the extended "phase space" (which is the usual phase space of concentrations augmented by 1 dimension for the time direction) corresponds to the time points at which the trajectory of one of the concentration phase space variables (in our case, coIII) exhibits a maximum. Thus, limit cycles manifest themselves as fixed points, period-2 cycles as period-2 points, tori as closed invariant loops, and so forth.

4. Case Studies

Example 1: The Hemin−Hydrogen Peroxide−Sulfite Oscillator. The hemin−hydrogen peroxide−sulfite oscillator is an example of an oscillatory system where the pH value of the reaction medium shows periodical changes. In this reaction system, hemin acts as a mimic for heme-containing enzymes and provides for a feedback mechanism that—together with autocatalysis—allows for oscillatory dynamics. Experimental results are reported in refs 25 and 26. The proposed reaction mechanism[27] accounts for most of the experimentally observed dynamics. It reads

$$\begin{aligned}
SO_3^{2-} + H^+ &\overset{k_5,k_4}{\rightleftharpoons} HSO_3^- \\
H_2O_2 + SO_3^{2-} &\xrightarrow{k_1} SO_4^{2-} + H_2O \\
H_2O_2 + HSO_3^- &\xrightarrow{k_2} SO_4^{2-} + H^+ + H_2O \\
H_2O_2 + HSO_3^- + H^+ &\xrightarrow{k_3} SO_4^{2-} + 2H^+ + H_2O \\
AH^+ &\overset{k_6,k_7}{\rightleftharpoons} A + H^+ \\
A &\xrightarrow{k_8} \text{products}
\end{aligned} \tag{19}$$

where AH^+ and A correspond to the hemin molecule carrying two aquo ligands or one aquo and one hydroxy group in its axial positions, respectively. The reaction mechanism (eq 19) consists of six chemical species and eight reaction steps. Four of the species (SO_3^{2-}, H_2O_2, H^+, and A) are supplied to a continuous-flow stirred tank reactor at a variable flow rate k_0 while all six chemical species are removed from the reactor at the same rate. Thus, there is a constant matter flow through the reactor which keeps the reaction system away from thermodynamic equilibrium. By changing the flow rate k_0 (between 1×10^{-4} and $4 \times 10^{-4}\ s^{-1}$), one can observe different dynamical behavior such as stationary (nonequilibrium) states, periodic oscillations, and burst oscillations.[27]

Assuming mass-action kinetics, the following system of ordinary differential equations is derived from (19):

$$\begin{aligned}
\dot{x}_1 &= -k_1x_1x_2 + k_4x_3 - k_5x_1x_4 + k_0(x_1^0 - x_1) \\
\dot{x}_2 &= -k_1x_1x_2 - k_2x_2x_3 - k_3x_2x_3x_4 + k_0(x_2^0 - x_2) \\
\dot{x}_3 &= -k_2x_2x_3 - k_3x_2x_3x_4 - k_4x_3 + k_5x_1x_4 - k_0x_3 \\
\dot{x}_4 &= k_2x_2x_3 + k_3x_2x_3x_4 + k_4x_3 - k_5x_1x_4 + k_6x_6 - k_7x_4x_5 + k_0(x_4^0 - x_4) \\
\dot{x}_5 &= k_6x_6 - k_7x_4x_5 - k_8x_5 + k_0(x_5^0 - x_5) \\
\dot{x}_6 &= -k_6x_6 + k_7x_4x_5 - k_0x_6
\end{aligned} \tag{20}$$

The parameters for the numerical integration are tabulated in Table 1. The correspondence between chemical species and phase space variables x_1, ... , x_6 is as follows: $x_1 \leftrightarrow SO_3^{2-}$, $x_2 \leftrightarrow H_2O_2$, $x_3 \leftrightarrow HSO_3^-$, $x_4 \leftrightarrow H^+$, $x_5 \leftrightarrow$ A, and $x_6 \leftrightarrow AH^+$. The concentrations of the substances in the inflow streams are denoted by x_i^0.

ODE system 20 can be rewritten in the compact vector notation

$$\dot{\mathbf{x}} = \mathbf{C}\cdot\mathbf{R}(\mathbf{x}, k) + k_0(\mathbf{x}^0 - \mathbf{x}) \tag{21}$$

where we introduce the matrix of stoichiometric coefficients **C** (without the in- and outflow terms) and the vector of reaction rates **R** as

$$\mathbf{C} = \begin{pmatrix} -1 & 0 & 0 & 1 & -1 & 0 & 0 & 0 \\ -1 & -1 & -1 & 0 & 0 & 0 & 0 & 0 \\ 0 & -1 & -1 & -1 & 1 & 0 & 0 & 0 \\ 0 & 1 & 1 & 1 & -1 & 1 & -1 & 0 \\ 0 & 0 & 0 & 0 & 0 & 1 & -1 & -1 \\ 0 & 0 & 0 & 0 & 0 & -1 & 1 & 0 \end{pmatrix} \mathbf{R} = \begin{pmatrix} k_1 x_1 x_2 \\ k_2 x_2 x_3 \\ k_3 x_2 x_3 x_4 \\ k_4 x_3 \\ k_5 x_1 x_4 \\ k_6 x_6 \\ k_7 x_4 x_5 \\ k_8 x_5 \end{pmatrix} \tag{22}$$

In the first step of the reduction process, we test for chemical constraints among the reactants, which are expressed by a nonmaximal rank of the stoichiometric matrix **C**. For system 20, we find that rank(**C**) = 4. We note that the two row vectors

$$\mathbf{v}_1{}^T = (1, -1, 1, 0, 0, 0)$$

$$\mathbf{v}_2{}^T = (0, 0, 1, 1, 0, 1)$$

satisfy

$$\mathbf{v}_1{}^T\cdot C = 0\cdot\mathbf{v}_1{}^T$$

$$\mathbf{v}_2{}^T\cdot C = 0\cdot\mathbf{v}_2{}^T$$

that is, $\mathbf{v}_1{}^T$ and $\mathbf{v}_2{}^T$ are left eigenvectors of the stoichiometric matrix **C** for the eigenvalue zero. Therefore, we chose the following linear coordinate transformation (eq 23) where the last two rows of the transformation matrix are just these left eigenvectors:

$$\begin{pmatrix} y_1 \\ y_2 \\ y_3 \\ y_4 \\ y_5 \\ y_6 \end{pmatrix} = \begin{pmatrix} 0 & 1 & 0 & 0 & 0 & 0 \\ 0 & 0 & 0 & 0 & 0 & 1 \\ 0 & 0 & 0 & 0 & 1 & 0 \\ 1 & 0 & 0 & 0 & 0 & 0 \\ 1 & -1 & 1 & 0 & 0 & 0 \\ 0 & 0 & 1 & 1 & 0 & 1 \end{pmatrix} \begin{pmatrix} x_1 \\ x_2 \\ x_3 \\ x_4 \\ x_5 \\ x_6 \end{pmatrix} \tag{23}$$

Thus, in the *y*-coordinate system, we achieve a splitting of the transformed ODE system into a 4-dimensional subsystem for the variables (y_1, ... , y_4) and a completely decoupled 2-dimensional subsystem for the variables y_5 and y_6:

$$\begin{aligned} \dot{y}_1 &= -r_1(y) - r_2(y) - r_3(y) + k_0(x_2^0 - y_1) \\ \dot{y}_2 &= -r_6(y) + r_7(y) - k_0 y_2 \\ \dot{y}_3 &= -k_8 y_3 + r_6(y) - r_7(y) + k_0(x_5^0 - y_3) \\ \dot{y}_4 &= -r_1(y) + r_4(y) - r_5(y) + k_0(x_1^0 - y_4) \\ \dot{y}_5 &= k_0(x_1^0 - x_2^0 - y_5) \\ \dot{y}_6 &= k_0(x_4^0 - y_6) \end{aligned} \tag{24}$$

where $r_i(y) \equiv R_i(x(y))$ and the functions $x(y)$ are given by the inverse of (23). Due to the choice of the linear transformation (eq 23), the last two equations in (24) only depend on the in- and outflow terms proportional to k_0. They can easily be integrated and yield the following solution for zero initial condition:

$$\begin{aligned} y_5(t) &= (x_1^0 - x_2^0)(1 - \exp(-k_0 t)) \\ y_6(t) &= (x_4^0)(1 - \exp(-k_0 t)) \end{aligned} \tag{25}$$

with

$$\lim_{t\to\infty} y_5(t) = x_1^0 - x_2^0 =: y_5^\infty$$

$$\lim_{t\to\infty} y_6(t) = x_4^0 =: y_6^\infty$$

Thus, after a transient time of order $1/k_0$, the trajectories of system 24 relax to a 4-dimensional attracting manifold given by

$$y_5 = y_5^\infty, \quad y_6 = y_6^\infty \tag{26}$$

where the essential asymptotic dynamics takes place.

Indeed, numerical simulations of the (y_1, y_2, y_3, y_4)-subsystem of (24) with y_5 and y_6 being replaced by their constant asymptotic values (eq 26) show that the resulting time series are virtually identical to those obtained for the full 6-dimensional system (eq 24) after an initial transient phase. By assigning constant values to y_5 and y_6, we place the system from the very beginning on a 4-dimensional manifold and neglect the (transient) approach of the trajectories toward that manifold.

We note that by rewriting the equations of (26) using *x*-coordinates and the correspondence between chemical species and phase space variables, one may provide a physical interpretation of these equations in terms of conservation laws. In particular, (27) and (28)

$$[SO_3{}^{2-}] - [H_2O_2] + [HSO_3{}^-] = [SO_3{}^{2-}]^0 - [H_2O_2]^0 \tag{27}$$

$$[HSO_3{}^-] + [H^+] + [AH^+] = [H^+]^0 \tag{28}$$

express the mass conservation of S atoms and H^+ ions, respectively. Here, one can recognize the left-hand sides of the equations as $\mathbf{v}_1{}^T\cdot\mathbf{x}$ (eq 27) and $\mathbf{v}_2{}^T\cdot\mathbf{x}$ (eq 28), while the right-hand sides denote the concentrations of the corresponding chemicals in the inflow streams.

So far, we have used the constraints (eq 26) given by the stoichiometric matrix **C** to identify redundant dynamical degrees of freedom, which led us to a 4-dimensional system. In the next step, we look for quasi-integrals as described in the second section of this article. As an example, consider the rate equation for x_1:

$$\dot{x}_1 = -k_1 x_1 x_2 + k_4 x_3 - k_5 x_1 x_4 + k_0(x_1^0 - x_1)$$

There are two potential quasi-integrals I_{ij} of the form of (8), namely,

$$I_{14}(x(t)) \equiv \frac{k_1 x_1(t) x_2(t)}{k_4 x_3(t)} \sim 1, \quad I_{45}(x(t)) \equiv \frac{k_4 x_3(t)}{k_5 x_1(t) x_4(t)} \sim 1 \tag{29}$$

Since the reaction rates in I_{ij} always appear with opposite signs,

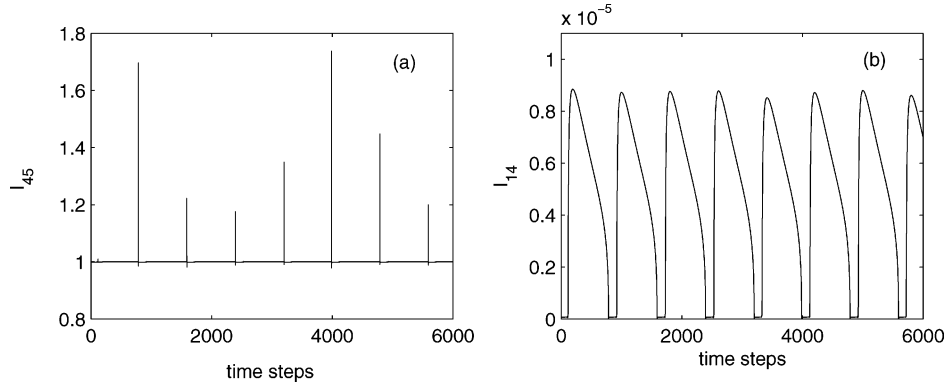

Figure 1. Ratios of reaction rates during the search for quasi-integrals in the hemin−hydrogen peroxide−sulfite oscillator. (a) $I_{45} = R_4/R_5 \sim 1$ approaches a constant value in the long-term limit and therefore defines a quasi-stationary manifold. (b) In contrast, $I_{14} = R_1/R_4$ remains a heavily oscillating function bounded away from 1 and therefore does not fulfill the condition for a quasi-integral. Note the scale difference of the axes for I_{45} and I_{14}.

we multiplied both sides of eq 8 by -1 to achieve the form of (29). By numerical simulations, we find that $I_{45}(x(t)) \sim 1$, while $I_{14}(x(t))$ remains a heavily oscillating function in the long time limit, as shown in Figure 1. This procedure is repeated for the other five rate equations (results not shown). However, additional quasi-integrals cannot be found. Note that it is not necessary to check the rate equation for $\dot{x}_2$ for quasi-integrals, since all reaction rates appear with the same (negative) sign.

Following the argumentation of Stiefenhofer,[22] we assume an embedding of the 4-dimensional ODE system into an ϵ-dependent family of systems such that $\tilde{I}_{45} = r_4(y) - r_5(y)$ becomes the dominant reaction step:

$$\begin{aligned}
\dot{y}_1 &= -r_1(y) - r_2(y) - r_3(y) + k_0(x_2^0 - y_1)\\
\dot{y}_2 &= -r_6(y) + r_7(y) - k_0 y_2\\
\dot{y}_3 &= -k_8 y_3 + r_6(y) - r_7(y) + k_0(x_5^0 - y_3)\\
\epsilon\dot{y}_4 &= r_4(y) - r_5(y) - \epsilon(r_1(y) + k_0(x_1^0 - y_4))
\end{aligned} \tag{30}$$

where ϵ is a small dimensionless quantity. After rescaling of time according to

$$\tau = \frac{t}{\epsilon} \tag{31}$$

and taking the limit $\epsilon \to 0$, we obtain the following ODE for the fast subsystem:

$$\frac{\mathrm{d}}{\mathrm{d}\tau} y_4 = r_4(y) - r_5(y) \tag{32}$$

Its stationary points, given by $r_4(y) - r_5(y) = 0$, define the quasi-stationary manifold:

$$k_4 \underbrace{(y_5^\infty - y_4 + y_1)}_{x_3} = k_5 \underbrace{y_4}_{x_1} \underbrace{(y_6^\infty - y_5^\infty - y_1 - y_2 + y_4)}_{x_4} \tag{33}$$

The occurrence of the small parameter ϵ in front of the time derivative of y_4 in (30) indicates that this quantity varies significantly only on short time scales and thereafter instantaneously follows the dynamics of the slow variables according to (33). Consequently, we have to solve the defining equation of the quasi-stationary manifold (eq 33) for nonnegative y_4. The solution of this quadratic equation is

$$\begin{aligned}
y_4 = \frac{1}{2}\left(y_5^\infty - y_6^\infty + y_1 + y_2 - \frac{k_4}{k_5}\right) +\\
\frac{1}{2}\sqrt{\left(y_5^\infty - y_6^\infty + y_1 + y_2 + \frac{k_4}{k_5}\right)^2 + 4\frac{k_4}{k_5}(y_6^\infty - y_2)}
\end{aligned} \tag{34}$$

where we must consider only the positive square root, since y_4 represents a concentration and therefore $y_4 \geq 0$ must hold. That (33) really defines an attracting quasi-stationary manifold can be checked by direct computation of the Jacobian along this manifold:

$$\begin{aligned}
\frac{\partial}{\partial y_4}(r_4 - r_5)|_{y_4 = y_4(y_1, y_2)} &= -k_4 - k_5(y_6^\infty - y_5^\infty - y_1 - y_2 + 2y_4)|_{y_4 = y_4(y_1, y_2)}\\
&= -k_5\sqrt{\left(y_5^\infty - y_6^\infty + y_1 + y_2 + \frac{k_4}{k_5}\right)^2 + 4\frac{k_4}{k_5}(y_6^\infty - y_2)}
\end{aligned}$$

On the other hand, it is known[28] that if the fast subsystem is entirely composed of reversible reactions, as it is in our case (r_4 and r_5 correspond to the first reversible reaction step in (19)), then its stationary points automatically define an attracting manifold for the original flow.

As a result of the QSSA using (33), we obtain the following 3-dimensional ODE system:

$$\begin{aligned}
\dot{y}_1 &= -r_1(y', y_4) - r_2(y', y_4) - r_3(y', y_4) + k_0(x_2^0 - y_1)\\
\dot{y}_2 &= -r_6(y') + r_7(y', y_4) + k_0(x_6^0 - y_2)\\
\dot{y}_3 &= -r_8(y') + r_6(y') - r_7(y', y_4) + k_0(x_5^0 - y_3)
\end{aligned} \tag{35}$$

where we have explicitly indicated the dependence of the reaction rates r_i on the collection of slow ($y' = \{y_1, y_2, y_3\}$) and fast (y_4) variables. Together with the algebraic relations (26) and (34), this 3-dimensional ODE system quantitatively reproduces the dynamical features of the original 6-dimensional one (eq 20), the details of which have been reported earlier.[27] We ascertained the validity of our approximation by comparing time series for the entire range of relevant values of the bifurcation parameter k_0. As a result, there are essentially no differences

TABLE 2: Detailed (BFSO) Model of the Peroxidase−Oxidase Reaction[32] [a]

reaction	R_i	rate constant k_i [b]
(1) NADH + O_2 + H^+ → NAD^+ + H_2O_2	k_1[NADH][O_2]	3.0 [c]
(2) H_2O_2 + Per^{3+} → coI + H_2O	k_2[H_2O_2][Per^{3+}]	1.8×10^7 [c]
(3) coI + NADH → coII + $NAD^•$	k_3[coI][NADH]	4.0×10^4 [c]
(4) coII + NADH → Per^{3+} + $NAD^•$	k_4[coII][NADH]	2.6×10^4 [c]
(5) $NAD^•$ + O_2 → NAD^+ + O_2^-	k_5[$NAD^•$][O_2]	2.0×10^7 [c]
(6) O_2^- + Per^{3+} → coIII	k_6[O_2^-][Per^{3+}]	1.7×10^7 [c]
(7) $2O_2^-$ + $2H^+$ → H_2O_2 + O_2	k_7[O_2^-]^2	5.0×10^6 [c]
(8) coIII + $NAD^•$ → coI + NAD^+	k_8[coIII][$NAD^•$]	1.35×10^8 [c]
(9) $2NAD^•$ → NAD_2	k_9[$NAD^•$]^2	5.6×10^7 [c]
(10) Per^{3+} + $NAD^•$ → Per^{2+} + NAD^+	k_{10}[Per^{3+}][$NAD^•$]	1.8×10^6 [c]
(11) Per^{2+} + O_2 → coIII	k_{11}[Per^{2+}][O_2]	1.0×10^5 [c]
(12) → NADH	k_{12}	variable [d]
(13) O_2(gas) → O_2(liquid)	$k_{13}[O_2]_{eq}$	6.0×10^{-3} [e,f]
(−13) O_2(liquid) → O_2(gas)	k_{-13}[O_2]	6.0×10^{-3} [e]

[a] The rate constants are taken from ref 33. [b] The concentrations of H^+ are taken to be constant and absorbed into the rate constants k_i, since the reaction system runs in a buffer solution at pH 6.3. [c] In M^{-1} s^{-1}. [d] Between 1.0×10^{-7} and 1.345×10^{-7} M s^{-1}. [e] In s^{-1}. [f] The value of $[O_2]_{eq}$ is 1.2×10^{-5} M.

between the dynamics produced by the 6- and the 3-dimensional models. This conclusion is further supported by virtually identical bifurcation diagrams for both systems (not shown).

Example 2: The Peroxidase−Oxidase Reaction. The peroxidase−oxidase reaction is the prototypical example of an oscillatory enzyme system (for a review, see ref 29). Considerable experimental effort has been devoted to identifying the individual reaction steps that occur in this reaction system (reviewed in ref 30). At the same time, a series of theoretical investigations has been conducted to reproduce the observed type of dynamics in numerical simulations (reviewed in ref 31). The starting point of our analysis is a reaction mechanism proposed by Bronnikova, Fed'kina, Schaffer, and Olsen[32] (Table 2) that shows periodic mixed-mode oscillations as well as (homoclinic) chaos.[33,34] It comprises 14 individual reaction steps and 10 species, yielding a 10-dimensional ODE system based on mass-action kinetics:

$$
\begin{aligned}
\dot{x}_1 &= k_2 x_4 x_{10} - k_3 x_1 x_6 + k_8 x_3 x_5 \\
\dot{x}_2 &= k_3 x_1 x_6 - k_4 x_2 x_6 \\
\dot{x}_3 &= -k_8 x_3 x_5 + k_{11} x_7 x_9 + k_6 x_8 x_{10} \\
\dot{x}_4 &= k_1 x_6 x_7 + k_7 x_8^2 - k_2 x_4 x_{10} \\
\dot{x}_5 &= k_3 x_1 x_6 + k_4 x_2 x_6 - k_5 x_5 x_7 - k_8 x_3 x_5 - 2k_9 x_5^2 - k_{10} x_5 x_{10} \\
\dot{x}_6 &= -k_1 x_6 x_7 - k_3 x_1 x_6 - k_4 x_2 x_6 + k_{12} \\
\dot{x}_7 &= -k_1 x_6 x_7 - k_5 x_5 x_7 + k_7 x_8^2 - k_{11} x_7 x_9 - k_{-13} x_7 + k_{13}[O_2]_{eq} \\
\dot{x}_8 &= k_5 x_5 x_7 - 2k_7 x_8^2 - k_6 x_8 x_{10} \\
\dot{x}_9 &= k_{10} x_5 x_{10} - k_{11} x_7 x_9 \\
\dot{x}_{10} &= -k_2 x_4 x_{10} + k_4 x_2 x_6 - k_6 x_8 x_{10} - k_{10} x_5 x_{10}
\end{aligned}
\tag{36}
$$

The parameter values for our simulations as well as the oxygen concentration $[O_2]_{eq}$ at equilibrium between the gas/liquid phase are taken from ref 33 and are compiled in Table 2. We used zero initial values for all species except for x_{10}^0, which was set to the total enzyme concentration of 1.5×10^{-6} M. k_{12} was taken as the bifurcation parameter ranging between 1.00×10^{-7} and 1.34×10^{-7} M s^{-1}. The correspondence between phase space variables x_1, ... , x_{10} and chemical species is as follows: $x_1 \leftrightarrow Per^{5+}$ (or coI), $x_2 \leftrightarrow Per^{4+}$ (or coII), $x_3 \leftrightarrow Per^{6+}$ (or coIII), $x_4 \leftrightarrow H_2O_2$, $x_5 \leftrightarrow NAD^•$, $x_6 \leftrightarrow$ NADH, $x_7 \leftrightarrow O_2$, $x_8 \leftrightarrow O_2^-$, $x_9 \leftrightarrow Per^{2+}$, and $x_{10} \leftrightarrow Per^{3+}$. Per^{n+} denotes the different oxidation states of the enzyme peroxidase.

Before applying the algorithm for finding quasi-integrals, we can immediately eliminate one dynamical degree of freedom, since the rank of the stoichiometric matrix of ODE system 36 is 9. The consequential linear relationship between some of the chemical species can be taken as

$$x_9 = x_{10}^0 - x_{10} - x_3 - x_1 - x_2 \tag{37}$$

which simply means that the total amount of enzyme peroxidase is conserved in time. Note that the reduction from 10 to 9 dimensions does not lead to any information loss due to (37) being an exact conservation relation. Therefore, we shall treat the 9- and 10-dimensional systems on equal footing below. As in (29), we obtained three candidates for quasi-integrals in the PO system:

$$
\begin{aligned}
I_{127} &= \frac{R_1 + R_7}{R_2} \sim 1 \leftrightarrow x_4 \sim \frac{k_1 x_6 x_7 + k_7 x_8^2}{k_2 x_{10}} \\
I_{567} &= \frac{R_5}{R_6 + 2R_7} \sim 1 \leftrightarrow x_8 \sim -\frac{1}{4}\frac{k_6}{k_7} x_{10} + \sqrt{\frac{1}{16}\left(\frac{k_6}{k_7} x_{10}\right)^2 + \frac{1}{2}\frac{k_5}{k_7} x_5 x_7} \\
I_{34} &= \frac{R_3}{R_4} \sim 1 \leftrightarrow x_2 \sim \frac{k_3}{k_4} x_1
\end{aligned}
\tag{38}
$$

They are shown in Figure 2a−c (cf. Table 2 for the definition of the R_i). In I_{127} and I_{567}, we needed to balance three terms for obtaining approximately constant functions. In particular, Figure 2d shows that it is not enough to balance only R_1 with R_2, because there are time intervals where I_{12} shows large deviations from the constant value 1. The attractivity of the manifolds (eq 38) is evident from direct calculation of the corresponding Jacobian, and the application of the QSSA for x_4, x_8, and x_2 yields successively an 8-, 7-, and finally the following 6-dimensional ODE system in the original x-variables:

$$
\begin{aligned}
\dot{x}_1 &= k_1 x_6 x_7 + k_7 x_8^2 - k_3 x_1 x_6 + k_8 x_3 x_5 \\
\dot{x}_3 &= k_6 x_{10} x_8 - k_8 x_5 x_3 + k_{11} x_7 x_9 \\
\dot{x}_5 &= 2k_3 x_1 x_6 - k_5 x_5 x_7 - k_8 x_3 x_5 - 2k_9 x_5^2 - k_{10} x_5 x_{10} \\
\dot{x}_6 &= -k_1 x_6 x_7 - 2k_3 x_1 x_6 + k_{12} \\
\dot{x}_7 &= -k_1 x_6 x_7 - k_5 x_5 x_7 + k_7 x_8^2 - k_{11} x_7 x_9 - k_{-13} x_7 + k_{13}[O_2]_{eq} \\
\dot{x}_{10} &= -k_1 x_6 x_7 - k_7 x_8^2 + k_3 x_1 x_6 - k_6 x_{10} x_8 - k_{10} x_5 x_{10}
\end{aligned}
\tag{39}
$$

where x_8 in (39) still has to be replaced by its expression in the second equation of (38). To compare the dynamics of the reduced systems with the original one, we calculated Poincaré maps of successive maxima of the coIII concentration as the NADH inflow rate k_{12} is continuously varied. This procedure yields local bifurcation diagrams which resemble those from ref 34 due to a similar choice of parameter sets.

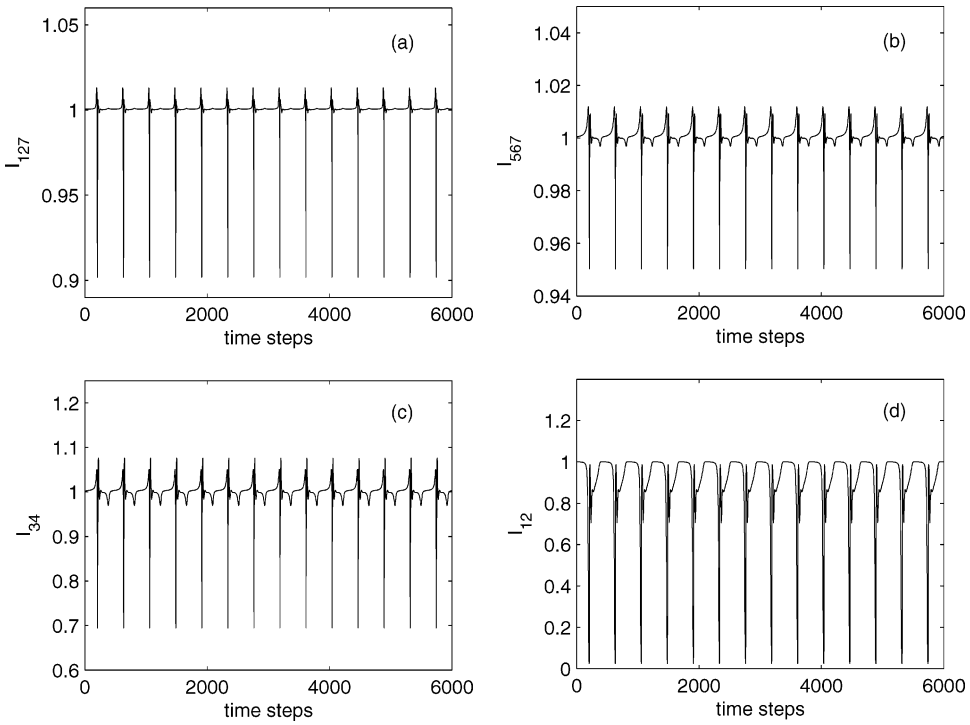

Figure 2. Quasi-integrals in the peroxidase−oxidase system. There are three possible candidates for quasi-stationary manifolds given by I_{127} (a), I_{567} (b), and I_{34} (c). I_{12} (d) shows that sometimes it is not sufficient to balance only two reaction steps to find a quasi-integral: compare with I_{127} (a), where three reaction steps have been used for the balance.

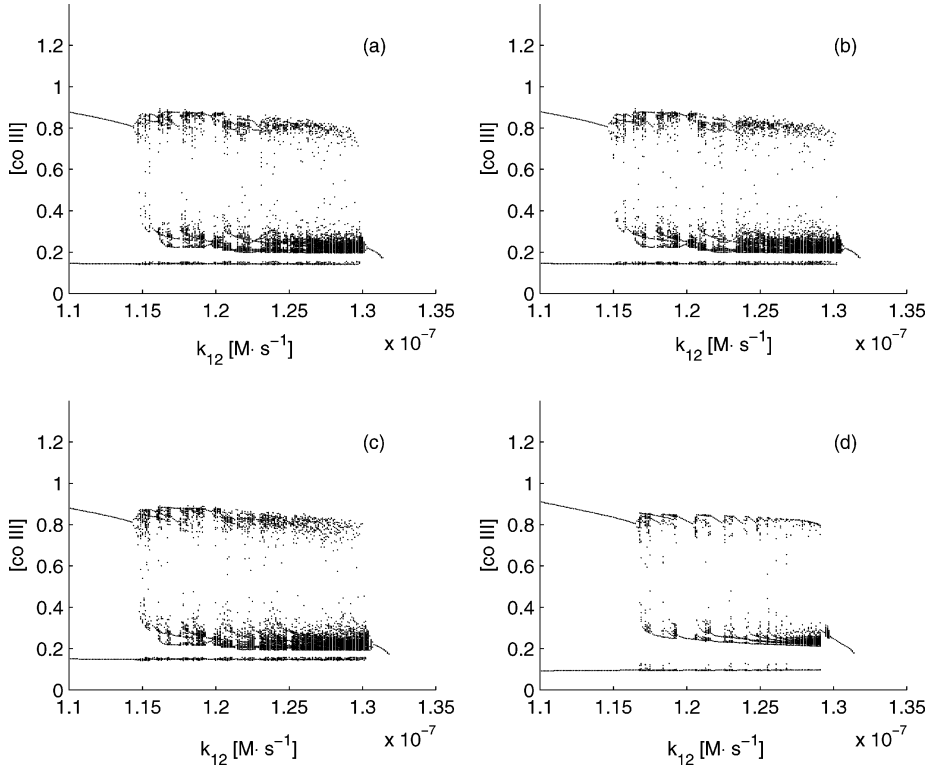

Figure 3. Bifurcation diagrams showing the maxima of peroxidase compound III (coIII) concentration as the NADH inflow rate k_{12} is varied: the original 10-/9-dimensional system (a); the 8-dimensional system (using $I_{127} \sim 1$) (b); the 7-dimensional system (using $I_{567} \sim 1$) (c); the 6-dimensional system (using $I_{34} \sim 1$) (d). The mixed-mode states as well as the alternating periodic and chaotic windows appear in all of the reduced systems (b−d) but at slightly different parameter values (d). The chaotic windows are less pronounced in the 6-dimensional reduced system (d).

Let us now address the most prominent dynamical changes that are observed during the successive reduction from a 10-variable to a 6-variable ODE system. Our analysis is based on a qualitative agreement of the bifurcation scenarios in the different versions of the reaction model; a detailed quantitative investigation is beyond the scope of the present article, in which we mainly focus on the demonstration of the method of quasi-integrals. Figure 3a shows the bifurcation scenario in the 10/9-dimensional system, as it has already been investigated in ref 33. Of particular interest are the mixed-mode states L^S. (The notation L^S denotes a periodic oscillatory state where one period consists of L large and S small amplitude oscillations.) The

mixed-mode states as well as the alternating periodic and chaotic windows are clearly preserved throughout the reduction procedure. The bifurcation scenarios for the reduced 8- and 7-dimensional systems are in very good quantitative agreement with the original 10/9-dimensional one (Figure 3b,c). This finding is also supported by nearly coinciding time series with respect to amplitude and frequency of the oscillations and by nearly identical 3-dimensional projections of the phase portrait. It is only for the 6-dimensional system that we find some quantitative deviations from the original dynamical behavior, as the amplitude and frequencies of the oscillations are slightly altered. There, we also observe a shift in parameter space where the first chaotic and subsequent mixed-mode states emerge (Figure 3d). Moreover, the domains of chaotic dynamics are less pronounced, but it seems that the resolution of the periodic windows between two chaotic ones is increased.

The chemical interpretation of the quasi-integrals (eq 38) leads to surprising insights on the role of the two oxygen species O_2^- (x_8) and H_2O_2 (x_4) in the PO mechanism[32] (Table 2). From I_{127} and I_{567}, it becomes evident that the ratios of production and consumption of O_2^- and H_2O_2, respectively, are nearly constant throughout the reaction. Consequently, these two species can be considered as quasi-stationary, so that molecular oxygen O_2 (x_7) remains the only dynamical oxygen-containing species. A similar but less surprising argument applies to the quasi-integral I_{34} which shows that Per^{4+} (x_2) does not accumulate during the reduction

$$\mathrm{coI}\ (x_1) \xrightarrow{+e^-} \mathrm{coII}\ (x_2) \xrightarrow{+e^-} \mathrm{Per}^{3+}\ (x_{10}) \qquad (40)$$

since its production via R_3 is effectively compensated by its consumption in R_4.

5. Discussion

In this work, we present a numerical method for systematically finding quasi-stationary manifolds of a particular class in chemical reaction networks. It is shown that quasi-integrals of the form of (8) and (12) may arise from certain ratios of components of the reaction rate vector. Thus, the class of quasi-stationary manifolds that may be detected not only includes linear relationships among the phase space variables but generically also contains those which are defined by nonlinear equations. The crucial step in identifying a quasi-integral is to define under which conditions the graph of a quasi-integral is to be regarded as nearly constant. Especially for higher dimensional ODE systems, it would be of great value to have a numerical measure which allows for a more systematic identification of quasi-integrals. On the basis of some common properties, we suggest the following working definition: a quasi-integral $I(x)$ is a nonconstant function of the phase space variables that is confined along the trajectories almost everywhere to a stripe around the value 1 (or -1) of adjustable thickness μ. This means that outliers are only allowed in time intervals of adjustable length δ which should be small compared to typical time scales in the system such as the period of the oscillations.

After we have decided whether a certain ratio I_{ij} is to be regarded as nearly constant, our method is quite similar to other semiobjective methods such as principal component analysis or even singular perturbation theory. For the former method, one has to decide how many modes to keep in order to reconstruct the original data based on the eigenvalue spectrum of a suitable covariance matrix. However, since there is no a priori interpretation of these modes, so is a rigorous measure indicating how many modes to retain. On the other hand, for singular perturbation theory to be valid, the singular perturbation parameter ϵ is required to be sufficiently small. In practical applications, though, ϵ may even become of order unity for some systems without leaving the range where singular perturbation theory provides a satisfactory approximation. Thus, for a particular system, one usually relies on numerical simulations in order to test the validity of the approximation. Indeed, this is exactly what we do, having identified a possible candidate for a quasi-stationary manifold by visual inspection of the time series $I(x(t))$ of a quasi-integral $I(x)$ (Figures 1 and 2).

We have demonstrated our method using the 6-dimensional hemin and 10-dimensional PO systems. The reaction mechanism (eq 19) of the hemin system comprises two equilibria, and it is not too surprising that one of them corresponds to the quasi-integral we found. The QSSA seems to be appropriate and yields a 3-dimensional ODE system (eq 35), which quantitatively agrees with the dynamical properties of the original 6-dimensional mechanism (eq 20). In contrast, the PO reaction system is almost exclusively composed of irreversible reaction steps. Nevertheless, three possible candidates for quasi-stationary manifolds (eq 38) could be identified by the method of quasi-integrals, thus demonstrating that the method works not only for reaction mechanisms containing equilibria. Furthermore, two of the quasi-integrals yielded very good quantitative 8- and 7-dimensional approximations to the original dynamics, whereas there are slight changes in the parameter values where the bifurcations in the reduced 6-dimensional system occur. The reason for this behavior may be seen in the much larger deviations of the quasi-integral I_{34} from the constant value 1 as compared to I_{127} and I_{567} (Figure 2), indicating that the manifold defined by $I_{34} \sim 1$ is not as "quasi-stationary" as both of the other ones.

In summary, the method of quasi-integrals has been successfully applied to both a system containing fast equilibrium reactions and a reaction mechanism with rapidly equilibrating irreversible reaction steps. To fully appreciate its scope, the method should be tested for other reaction networks. In particular, our method is not restricted to mass-action kinetics; it can be easily applied to other types of kinetics, too. The only requirement is that the right-hand side of eq 1 is of the form of (6), that is, a sum of terms with different signs, so that there is some chance that some reaction steps balance each other. Therefore, it is not relevant whether the components of the reaction rate vector **R** are simple monomials such as in the mass-action case or more complicated functions. Hence, the method of quasi-integrals should be applicable to a broad spectrum of reaction mechanisms.

In conclusion, we conjecture that quasi-integrals are a valuable supplement to existing methods for the reduction of chemical reaction mechanisms, such as the computational singular perturbation method, since it generically also detects nonlinear quasi-stationary manifolds which, in general, are hard to find analytically.

Acknowledgment. We would like to thank Janos Tóth and Andrea Halmschlager (Budapest University of Technology and Economics, Department of Mathematical Analysis) for stimulating discussions. Financial support by the BMBF program CELLECT is gratefully acknowledged.

References and Notes

(1) Michal, G. *Biochemical pathways*; Spectrum: Heidelberg, Germany, 1999.

(2) Keener, J.; Sneyd, J. *Mathematical Physiology*; Springer: New York, 1998.
(3) Warneck, P. *Phys. Chem. Chem. Phys.* **1999**, *1*, 5471.
(4) Geiger, H.; Barnes, I.; Becker, K. H.; Bohn, B.; Brauers, T.; Donner, B.; Dorn, H.-P.; Elend, M.; Freitas Dinis, C. M.; Grossmann, D.; Hass, H.; Hein, H.; Hoffmann, A.; Hoppe, L.; Hülsemann, F.; Kley, D.; Klotz, B.; Libuda, H. G.; Maurer, T.; Mihelcic, D.; Moortgat, G. K.; Olariu, R.; Neeb, P.; Poppe, D.; Ruppert, L.; Sauer, C. G.; Shestakov, O.; Somnitz, H.; Stockwell, W. R.; Thüner, L. P.; Wahner, A.; Wiesen, P.; Zabel, F.; Zellner, R.; Zetzsch, C. *J. Atmos. Chem.* **2002**, *42*, 323.
(5) Allara, D. L.; Edelson, D. *Int. J. Chem. Kinet.* **1975**, *7*, 479.
(6) Warnatz, J. *Pure Appl. Chem.* **2000**, *72*, 2101.
(7) Györgyi, L.; Turányi, T.; Field, R. J. *J. Phys. Chem.* **1990**, *94*, 7162.
(8) Aguda, B. D.; Clarke, B. L. *J. Chem. Phys.* **1987**, *87*, 3461.
(9) Eiswirth, M.; Freund, A.; Ross, J. *Adv. Chem. Phys.* **1991**, *80*, 127.
(10) Hung, Y.-F.; Schreiber, I.; Ross, J. *J. Chem. Phys.* **1995**, *99*, 1980.
(11) Clarke, B. L. *Adv. Chem. Phys.* **1980**, *43*, 1.
(12) Turányi, T. *J. Math. Chem.* **1990**, *5*, 203.
(13) Price, N. D.; Reed, J. L.; Papin, J. A.; Wiback, S. J.; Palsson, B. O. *J. Theor. Biol.* **2003**, *225*, 185.
(14) Vajda, S.; Turányi, T. *J. Phys. Chem.* **1986**, *90*, 1664.
(15) Fenichel, N. *J. Differ. Equat.* **1979**, *31*, 53.
(16) Tichonov, A. N. *Mat. Sb.* **1952**, *31*, 575.
(17) O'Malley, R. E. *Singular Perturbation Methods for Ordinary Differential Equations*; Springer: New York, 1991; p 83.
(18) Li, G.; Tomlin, A. S.; Rabitz, H.; Tóth, J. *J. Chem. Phys.* **1993**, *99*, 3562.
(19) Roussel, M. R.; Fraser, S. J. *Chaos* **2001**, *11*, 196.
(20) Lam, S. H. *Combust. Sci. Technol.* **1993**, *89*, 375.
(21) Lin, C. C.; Segel, L. A. *Mathematics Applied to Deterministic Problems in the Natural Sciences*; SIAM: Philadelphia, PA, 1994.
(22) Stiefenhofer, M. *J. Math. Biol.* **1998**, *36*, 593.
(23) Ermentrout, B. *Simulating, Analyzing and Dynamical Systems: A Guide to XPPAUT for Researchers and Students*; SIAM: Philadelphia, PA, 2002. http://www.math.pitt.edu/[IMAGE]bard/xpp/xpp.html.
(24) Kuznetsov, Y. *Elements of Applied Bifurcation Theory*; Springer: Heidelberg, Germany, 1998.
(25) Hauser, M. J. B.; Strich, A.; Bakos, R.; Nagy-Ungvárai, Zs.; Müller, S. C. *Faraday Discuss.* **2001**, *120*, 229.
(26) Hauser, M. J. B.; Fricke, N.; Storb, U.; Müller, S. C. *Z. Phys. Chem.* **2002**, *216*, 375.
(27) Straube, R.; Müller, S. C.; Hauser, M. J. B. *Z. Phys. Chem.* **2003**, *217*, 1427.
(28) Schuster, S.; Schuster, R. *J. Math. Chem.* **1989**, *3*, 25.
(29) Hauser, M. J. B.; Olsen, L. F. In *Transport versus Structure—Their Competitive Roles in Biophysics and Chemistry*; Müller, S. C., Parisi, P., Zimmermann, W., Eds.; Springer: Heidelberg, Germany, 1999; p 252.
(30) Scheeline, A.; Olson, D. L.; Williksen, E. P.; Horras, G. A.; Klein, M. L.; Larter, R. *Chem. Rev.* **1997**, *97*, 793.
(31) Larter, R.; Olsen, L. F.; Steinmetz, C. G.; Geest, T. In *Chaos in Chemical and Biological Systems*; Field, R. J., Györgyi, L., Eds.; World Scientific: Singapore, 1993; p 175.
(32) Bronnikova, T. V.; Fed'kina, V. R.; Schaffer, W. M.; Olsen, L. F. *J. Phys. Chem.* **1995**, *99*, 9309.
(33) Hauser, M. J. B.; Olsen, L. F. *J. Chem. Soc., Faraday Trans.* **1996**, *92*, 2857.
(34) Hauser, M. J. B.; Olsen, L. F.; Bronnikova, T. V.; Schaffer, W. M. *J. Phys. Chem. B* **1997**, *101*, 5075.